Organic Geochemistry 167 (2022) 104405

Contents lists available at ScienceDirect

Organic Geochemistry

journal homepage: www.elsevier.com/locate/orggeochem

Distinct sources of bacterial branched GMGTs in the Godavari River basin (India) and Bay of Bengal sediments

Frédérique M.S.A. Kirkels [a,*], Muhammed O. Usman [b,1], Francien Peterse [a]

[a] Department of Earth Sciences, Utrecht University, Princetonlaan 8a, 3584 CB Utrecht, the Netherlands
[b] Geological Institute, ETH Zürich, Sonneggstrasse 5, 8092 Zürich, Switzerland

ARTICLE INFO

Associate Editor—**Isla S. Castañeda**

Keywords:
BrGMGTs
H-shaped brGDGTs
India
Godavari Basin
Bay of Bengal
Marine production

ABSTRACT

Branched glycerol monoalkyl glycerol tetraethers (brGMGTs) are a group of membrane-spanning lipids produced by (yet) unidentified bacteria. They are characterized by a C-C bond connecting the two alkyl chains, which is thought to enhance membrane stability at higher temperatures. So far, they have been found in peats, lakes, and marine sediments, where their abundance relative to that of branched glycerol dialkyl glycerol tetraethers (brGDGTs) increases with temperature. However, the preferred niche(s) for production and the origin of brGMGTs in the terrestrial and marine realm remain unknown. Here we explore the occurrence of brGMGTs in soils, suspended particulate matter (SPM) and riverbed sediments in the Godavari River basin, and compare these with brGMGTs in a Holocene sediment core from the Bay of Bengal close to the Godavari River mouth. BrGMGTs are mostly detected in agricultural and/or regularly inundated soils, and in the river at sites with standing water and/or agricultural/wastewater effluents, as well as in the delta, where low oxygen conditions and/or high nutrient levels prevail. In contrast, brGMGTs are continuously present in the marine sediment core, but with a different isomeric composition than in the terrestrial realm, indicating a primarily marine source. The stable brGMGT distribution downcore and brGMGT-inferred temperature estimates which resemble the bottom water temperature, may suggest marine brGMGT production in the deep water column and/or sediments. However, to establish the proxy potential of brGMGTs for paleoreconstructions in the terrestrial and marine realm, brGMGT sources and environmental controls require further study.

1. Introduction

Our understanding of past climate change is mostly based on sea surface temperature reconstructions, whereas fewer records exist for the terrestrial realm. This is largely due to the fact that continuous, high resolution sedimentary archives are relatively scarce on land. As an alternative, continental shelf sediments that receive large terrestrial inputs can be used to reconstruct past climate evolution on the nearby continent, for example by using land-derived lipid biomarkers, such as plant leaf waxes including *n*-alkyl compounds such as *n*-alkanes, *n*-alkanols, *n*-alkanoic acids and wax esters or terpenoids, lignin and sterols, preserved in these sediments (e.g., Pancost and Boot, 2004; Schefuß et al., 2005; Dubois et al., 2014; Li et al., 2020). Similarly, branched glycerol dialkyl glycerol tetraethers (brGDGTs), which are membrane lipids originally thought to be produced by soil bacteria (Weijers et al., 2007a), have been routinely employed as a continental paleothermometer (Weijers et al., 2007b; Dearing Crampton-Flood et al., 2018) based on empirical observations that the molecular structure of brGDGTs in soils worldwide changes with the mean annual air temperature (MAAT) and pH of their living environment (Weijers et al., 2007a; De Jonge et al., 2013; 2014a). BrGDGTs have also been proposed as tracers for the land to sea transport of soil organic carbon (OC) (Hopmans et al., 2004; Kirkels et al., 2020a), based on the assumption that they are produced in soils and transported by rivers following erosion. However, the use of brGDGT proxies has been challenged by more recent findings that brGDGTs are not exclusively soil-derived but that they are also produced in aquatic environments including rivers, lakes and coastal marine settings (Peterse et al., 2009; Tierney and Russell, 2009; Zell et al., 2013a,b; De Jonge et al., 2014b). As a consequence, it remains challenging to determine the relative contribution of soil-derived and aquatic-produced brGDGTs in sedimentary settings, complicating the application of brGDGT-based proxies for

* Corresponding author.
E-mail address: f.m.s.a.kirkels@uu.nl (F.M.S.A. Kirkels).
[1] Present address: Department of Physical & Environmental Sciences, University of Toronto Scarborough, Toronto, Ontario M1C1A4, Canada.

https://doi.org/10.1016/j.orggeochem.2022.104405
Received 9 September 2021; Received in revised form 10 February 2022; Accepted 9 March 2022
Available online 12 March 2022

reconstruction of environmental conditions on the nearby land.

A less commonly studied group of membrane lipids consists of the so-called H-shaped brGDGTs, or branched glycerol monoalkyl glycerol tetraethers (brGMGTs; Fig. 1). Like brGDGTs, the producers of brGMGTs are also still elusive, but brGMGTs differ from brGDGTs by having an additional covalent carbon–carbon bond that links the two alkyl chains and gives the compound its characteristic H-shape (Fig. 1a).

Liu et al. (2012) first identified an acyclic brGMGT with $[M + H]^+$ ions at *m/z* 1020 (aptly labelled H1020) in a semi-global range of marine surface sediments. Subsequently, Xie et al. (2014) found this compound in suspended particulate matter (SPM) from the oxygen minimum zone of the eastern Pacific, suggesting a marine source, likely anaerobic planktonic microbes. More recently, Naafs et al. (2018) also detected brGMGTs with one (H1034) or two (H1048) additional methylations in modern tropical peats and argued for their production in the anoxic, water-saturated subsurface layer. Tang et al. (2021) also found brGMGTs H1020, H1034 and H1048 in Late Quaternary peat cores from northeastern China, while Lü et al. (2019) reported on brGMGTs in Chinese coastal wetland sediments. Baxter et al. (2019) further identified several brGMGT isomers (H1020a,b,c, H1034a,b,c and H1048) in a suite of East African lake sediments.

Detailed investigation of brGMGTs in and around Lake Chala, a permanently stratified crater lake in Africa, indicated that they are abundantly produced in the anoxic part of the water column, but that only the (fully anoxic) sediments host the full suite of brGMGT isomers, indicating that most of the production takes place there (Baxter et al., 2021). In contrast to brGDGTs, brGMGTs with cyclopentane moieties have so far not been discovered (e.g., Naafs et al., 2018; Baxter et al., 2019).

The abundance of brGMGTs relative to that of brGDGTs (expressed as %brGMGT) appears to relate to temperature in peats and lakes (Naafs et al., 2018; Baxter et al., 2019). This may be due to the characteristic covalent C–C bond that is thought to enhance membrane stability at higher environmental temperatures (Morii et al., 1998; Schouten et al.,

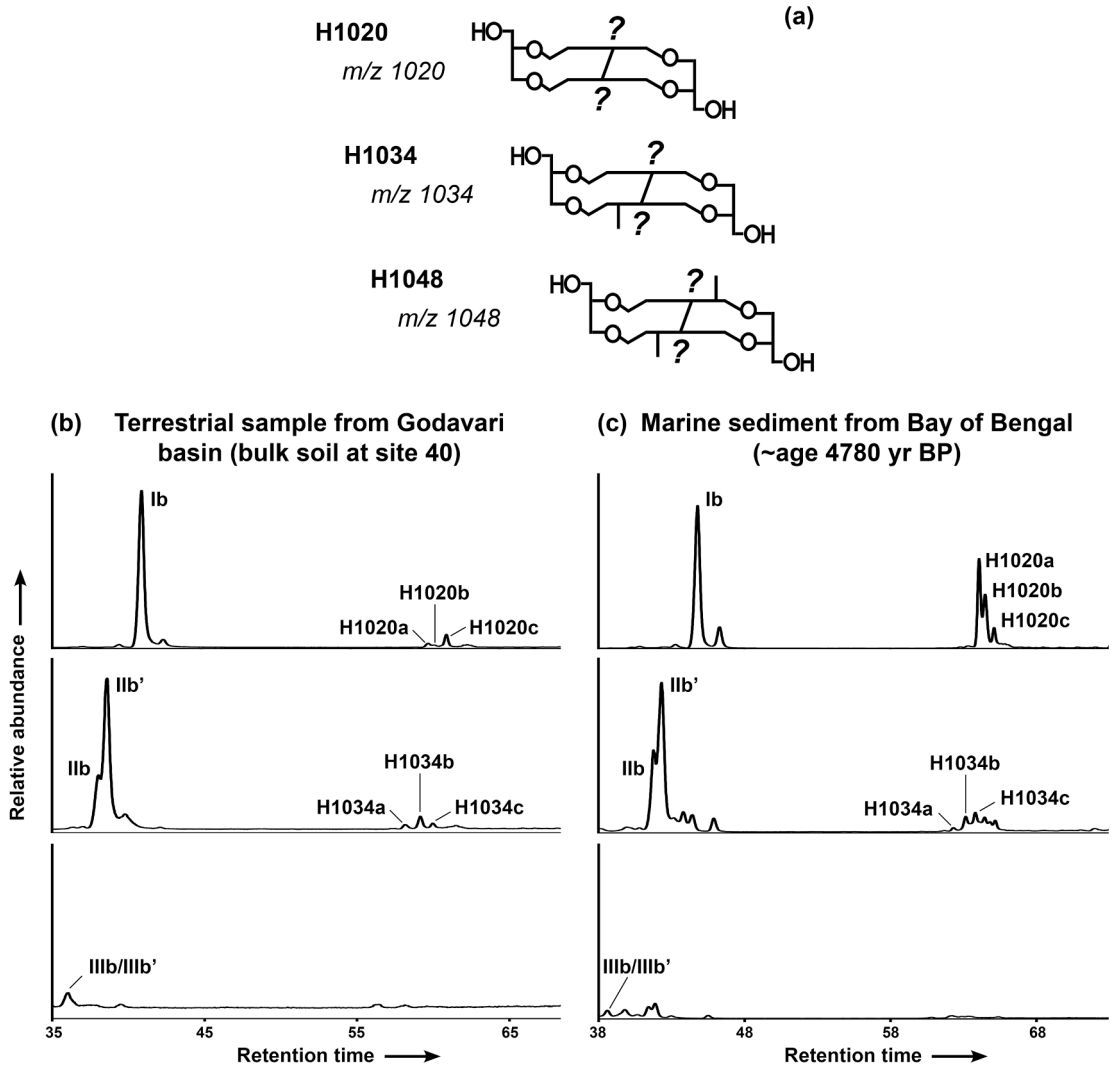

Fig. 1. (a) Tentative molecular structures of brGMGTs occurring at *m/z* 1020, 1034 and 1048 (after Naafs et al., 2018). Note that the exact location of the covalent C–C bond between the two alkyl chains is unknown. Terminology is according to Baxter et al. (2019), labelling them respectively as H1020, H1034 and H1048, with isomers indicated by a suffix letter (a–c) following the order in which they elute. Mass chromatograms for *m/z* 1020, 1034 and 1048 of the polar fraction of (b) (bulk) soil in the Godavari basin (at site 40) and (c) Holocene marine sediment in the Bay of Bengal (~4780 yr BP, 5.16–5.20 m depth below seafloor), with peaks indicating the occurring brGDGTs and brGMGTs. Peaks for H1048 are below the limit of detection for reliable integration. Notably, the retention time shows a small offset (~3 min.) between the terrestrial and marine samples due to their measurement at two UHPLC systems (at Utrecht University and NIOZ, respectively) using the same instrument settings. The chromatograms are representative of those found in the Godavari basin (i.e., terrestrial realm) and in Holocene marine sediments (i.e., marine realm), respectively.

2008). In addition, their degree of methylation (expressed as H-MBT; Naafs et al., 2018), and an index based on the relative abundances of (specific) brGMGT isomers correlates with MAAT (brGMGTI; Baxter et al., 2019). The presence of brGMGTs in ancient peat deposits and lignites (i.e., immature coal deposits) suggests that they are preserved at long(er) timescales and that they may be suitable to infer past climate change (Naafs et al., 2018; Inglis et al., 2019; Tang et al., 2021). Initial paleo-investigations from the marine realm revealed abundant brGMGTs in Paleocene and Eocene marine sediments from the Arctic (Sluijs et al., 2020) and southwest Pacific Ocean (Bijl et al., 2021). Although some trends can be recognized, the response of brGMGTs to presumed changes in reconstructed temperatures is not uniform among both sites. Where brGMGTs in the Arctic Ocean show an increase in % brGMGT and H-MBT (including all isomers) with MBT'$_{5me}$-based MAAT over the late Paleocene to early Eocene (Sluijs et al., 2020), brGMGTs in the southwest Pacific Ocean show no correlation with MBT'$_{5me}$-based MAAT for either of the proxies over the Maastrichtian-Rupelian interval (Bijl et al., 2021). In contrast, Bijl et al. (2021) found that the brGMGTI

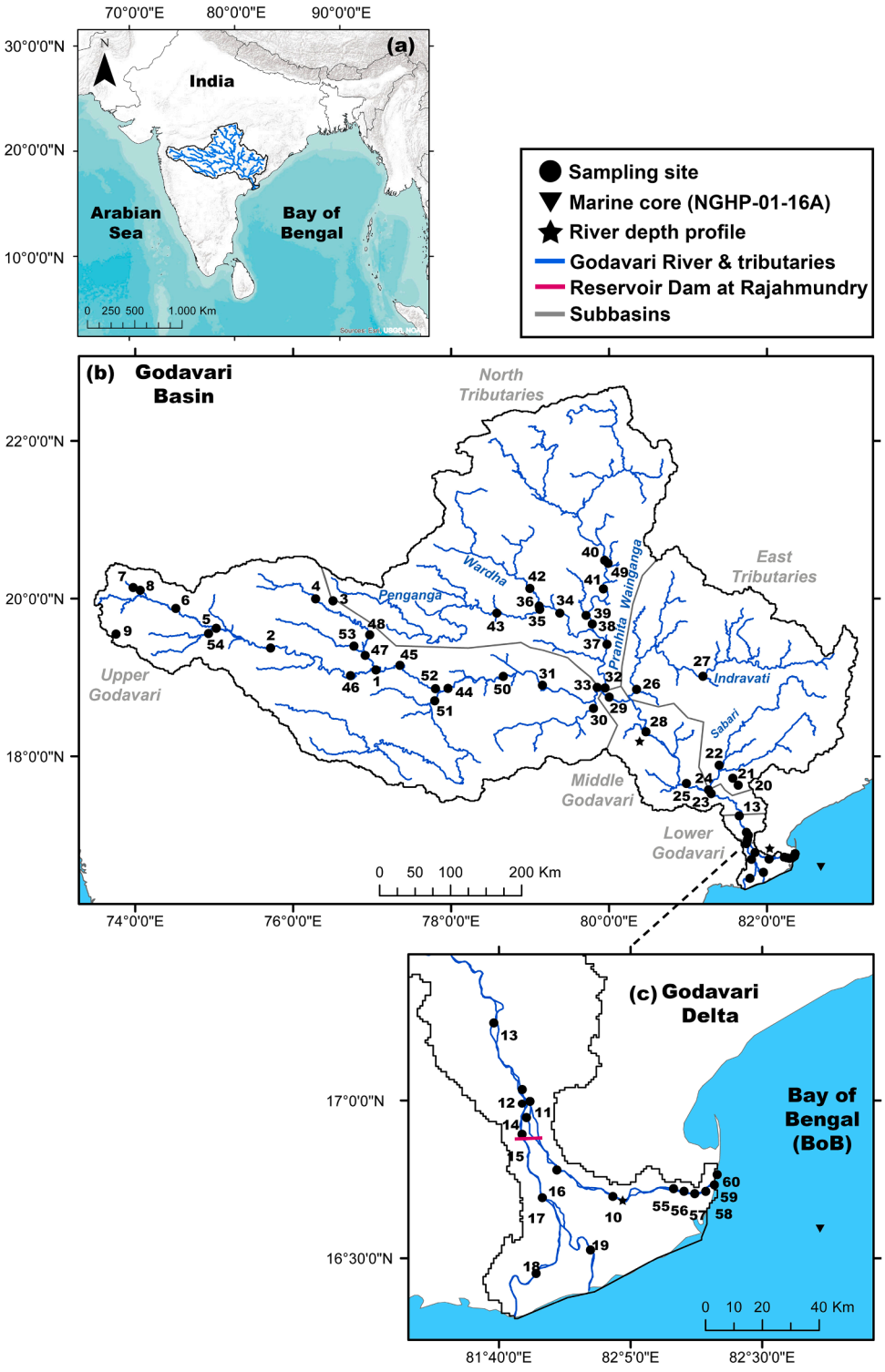

Fig. 2. (a) Location of the Godavari River basin in peninsular India. (b) Godavari River basin with sampling sites along the river (circle; the number indicates the site code), river depth profiles (star) and Holocene marine sediment core NGHP-01-16A (~1250 m water depth), retrieved ~ 40 km from the Godavari River mouth in the Bay of Bengal (triangle). Names of the subbasins (grey) and major rivers (blue) are indicated. (c) Zoom for the Godavari delta and the Reservoir Dam at Rajahmundry. (For interpretation of the references to colour in this figure legend, the reader is referred to the web version of this article.)

record for the Pacific Ocean resembled the trends in reconstructed MAAT and SST, whereas Sluijs et al. (2020) found no such correlations for brGMGTI in the Arctic Ocean record.

Regardless, the origin of brGMGTs in these sediment records (whether marine or terrestrial, soil or water column or sediment) is unresolved. Hence, the proxy potential of brGMGTs in marine sediments would benefit from a detailed evaluation of brGMGT distributions in modern samples along the soil-river-sea continuum. Moreover, the land-sea transport (mechanism) of brGMGTs has not yet been studied. Similarly, effects of hydrological dynamics (i.e., low/high flow conditions) and hydrodynamic sorting are unknown. As organic carbon and lipid biomarkers (e.g., fatty acids, *n*-alkanes, brGDGTs) are generally enriched in the fine grained sediment fraction due to associations with mineral surfaces, this may result in specific distributions with river depth (e.g., Galy et al., 2008; Freymond et al., 2018a; Kirkels et al., 2020a) as well as in differential transport, export, and burial efficiency of certain compounds in (marine) sedimentary records (e.g., Keil et al., 1997; Goñi et al., 2000; Bianchi et al., 2018; Freymond et al., 2018b; Yu et al., 2019; Hou et al., 2020; Kirkels et al., 2020a; Li et al., 2020; Eglinton et al., 2021).

Therefore, we here explore the occurrence and distribution of brGMGTs in soils, SPM, and in bulk and fine-grained (<63 μm) riverbed sediments collected in a dry and wet season in the Godavari River basin, the largest monsoon-fed river of peninsular India, to identify their main sources and production sites, and assess their transportation through the river basin. BrGMGTs are furthermore assessed along multiple river depth profiles and compared between bulk and fine fractions to gain insights into potential sorting and/or selective transport. Subsequently, brGMGTs were analysed in a Holocene marine sediment core retrieved from the Bay of Bengal in front of the Godavari River mouth to determine their transfer to the marine sedimentary archive.

2. Material and methods

2.1. Godavari Basin

The Godavari River is the largest monsoon-fed river and the second largest river of India behind the Ganges-Brahmaputra (catchment area: 3.1×10^5 km^2, length: 1465 km). It starts in the Western Ghats mountains and flows across peninsular India in a southeast direction, before emptying into the Bay of Bengal (Barbar and Kaplay, 2018) (Fig. 2a,b).

There are five subbasins: the Upper, Middle and Lower Godavari cover the main stem and drain 45% of the catchment area, while the other 55% is drained by the North Tributaries (Wainganga, Penganga, Wardha, Pranhita River) and East Tributaries (Indravati, Sabari River). The basin has marked dry and wet seasons, where the Southwest monsoon brings the majority of rainfall (>75%) in June–September (Barbar and Kaplay, 2018). The Godavari exports 94% of its annual discharge in this period (Biksham and Subramanian, 1988a,b). The Western Ghats act as an orographic barrier, strongly affecting rainfall distributions over peninsular India. As a result, the upper part of the Godavari basin, developed on Deccan basalts, is characterised by arid to semi-arid vegetation and receives limited precipitation (<1000 mm yr^{-1}), while moist and deciduous vegetation formed on felsic bedrocks and a higher annual precipitation (1000–2300 mm yr^{-1}) typify the lower basin (Babar and Kaplay, 2018). A few coal fields with active, open-pit mining exist in the North Tributary region (Singh et al., 2012; Pradhan et al., 2014).

Mean annual air temperatures range from 24.5 to 28 °C, with MAAT between 24.5 and 27 °C at a few elevated sites in the Western and Eastern Ghats mountain ranges (n = 8) and MAAT between 27 °C and 28 °C across most of the Godavari basin (average MAAT ± standard deviation: 27.2 ± 0.8 °C, n = 45) (Dearing Crampton-Flood et al., 2019). A major dam and Reservoir Lake at Rajahmundry control the flow to the tidally influenced delta (Fig. 2c). Here the river splits into three branches, where most of the discharge follows the northern branch through an estuary to the Bay of Bengal. Damming, particularly in the upper basin, has increased substantially over the last decades and controls the river flow year-round (Pradhan et al., 2014; Kirkels et al., 2020b).

2.2. Sample collection

Soils (0–10 cm) were collected during the dry season in February/March 2015 by removing the litter and combining 3–5 spatial replicates (n = 46). Both SPM and riverbed sediments were collected during the dry season (n = 18 and n = 37, respectively) as well as during the wet season in July/August 2015 (n = 40 and n = 37, respectively). For SPM, 10–80 L of water was collected at mid-channel position from bridges or a boat, or at 2–3 m out of the riverbank and filtered on pre-combusted glass fiber filters (0.7 μm, Whatman). River depth profiles (2 or 3 depths, 2 or 3 sites across river) were sampled in the Godavari delta (main branch) and in the main stem in the Middle Godavari in the wet season (Fig. 2b,c; sites 10 and 28). At these sites, additional subsurface river water containing SPM (n = 9) was collected at equal increments to the riverbed with a custom-built depth sampler (after Lupker et al., 2011). Riverbed sediments were retrieved from the middle of the river using either a Van Veen sediment sampler or a shovel when the water level was low. At selected sites, soils (n = 10) and wet season riverbed sediments (n = 25) were sieved to isolate the fine fraction (≤63 μm). All samples were stored frozen and subsequently freeze-dried. Bulk soils and riverbed sediments were homogenised prior to analysis. In total, 222 terrestrial samples were collected across the Godavari River basin.

A marine sediment core spanning the Early (n = 11) to Late Holocene (n = 35) was retrieved from the Bay of Bengal (NGHP expedition 01, 2006; Core NGHP-01-16A; 16.59331°N, 82.68345°E), ~40 km from the Godavari mouth and at 1268 m water depth. Sampling procedures and the age model were described by Ponton et al. (2012) and Usman et al. (2018).

2.3. Geochemical analyses

The total organic carbon content (%TOC) was determined after removal of inorganic carbon following van der Voort et al. (2016) for SPM, van Helmond et al. (2017) for bulk soils and sediments, Vonk et al. (2008) for fine soils and sediments, with an Elemental Analyser (SPM and bulk samples: Flash 2000, Thermo Scientific, at NIOZ, Texel, The Netherlands; fine samples: Flash 1112, Thermo Scientific, at VU University, Amsterdam, The Netherlands; analytical uncertainty < 0.1%). The total nitrogen content (%TN) was determined with an Elemental Analyser (bulk soils: Flash 2000; fine soils and sediments: Flash 1112) and an NCS Analyser (bulk sediments: NA 1500, Fisons Instruments, at Utrecht University, The Netherlands) (analytical uncertainty < 3%). Mineral surface area (MSA) of the bulk soils (n = 18), riverbed sediments (n = 10) collected in the dry season and the marine core (n = 46; n = 11 and n = 35 in Early and Late Holocene, respectively) were retrieved from Usman et al. (2018). Additional MSA analyses of bulk sediment collected in the dry (n = 1) and wet season (n = 11, mainly in the Godavari delta) were done following Usman et al. (2018). In brief, ~1 g of sample was combusted at 350 °C, subsequently degassed at the same temperature and then homogenised with agate and plastic mortar and pestle. The surface area was measured by the multi-point BET N_2 adsorption method using a Quantachrome Monosorb Analyser at ETH Zürich (analytical uncertainty < 1%).

2.4. BrGMGT extraction and analysis

The freeze-dried and homogenized soils (~2–20 g), riverbed sediments (~1–18 g) and SPM filters (cut into pieces, ~0.04–5 g) were extracted with an Accelerated Solvent Extractor (ASE 350, Dionex) at 100 °C and 7.6 × 10^6 Pa, using dichloromethane (DCM):methanol (MeOH) (9:1, v/v). The total lipid extracts (TLE) of the dry season SPM and all riverbed sediments were separated on an activated Al_2O_3 column into apolar, neutral and polar fractions, using hexane, hexane: dichloromethane (Hex:DCM; 1:1, v/v), DCM, and DCM:methanol (DCM: MeOH; 1:1, v/v) as eluents, respectively. TLEs of soils and wet season SPM were first saponified with KOH in MeOH (0.5 M) for 2 h at 70 °C. MilliQ water with NaCl was added and the neutral fraction was back-extracted with hexane (3 × 10 mL). This fraction was then dried over a Na_2SO_4 column and separated on an activated Al_2O_3 column into an apolar and polar fraction using hexane and DCM:MeOH (1:1, v/v) as eluents, respectively. The core samples were extracted according to Usman et al. (2018), and TLEs were further treated like the Godavari soils.

A known amount of internal standard (99 ng C_{46} GDGT; Huguet et al., 2006) was added to the polar fractions for quantification, after which all fractions were re-dissolved in hexane:isopropanol (99:1, v/v) and passed over a 0.45 μm polytetrafluoroethylene (PTFE) filter prior to analysis on an Agilent 1260 Infinity Ultrahigh Performance Liquid Chromatography (UHPLC) system coupled to an Agilent 6130 single quadrupole mass detector following the method of Hopmans et al. (2016). The brGMGTs were detected by their $[M + H]^+$ ions at *m/z* 1020, 1034 and 1048 and elute ~ 20 min later than brGDGTs with the same molecular mass. Identification of the different brGMGT isomers was achieved by comparison of peak retention time with that of known brGMGTs (Baxter et al., 2019). Peak area integration of brGMGTs was carried out using Chemstation. A peak area of 3 × 10^3 and a peak height 3 × the background was considered as the minimum for clearly defined peaks; smaller peaks were considered below detection limit.

2.5. Proxy calculations and statistics

The summed abundance of all brGMGTs relative to that of all brGDGTs is calculated following Naafs et al. (2018) including all known isomers:.

$$\%\text{brGMGT} = 100 \times (\Sigma\text{brGMGTs}/(\Sigma\text{brGMGTs} + \Sigma\text{brGDGTs})) \quad (1)$$

The degree of methylation of brGMGTs was calculated following Naafs et al. (2018), although adjusted to include all known isomers:.

$$\text{H-MBT} = (\text{H1020a} + \text{H1020b} + \text{H1020c})/(\text{H1020a} + \text{H1020b} + \text{H1020c} + \text{H1034a} + \text{H1034b} + \text{H1034c} + \text{H1048}) \quad (2)$$

As only acyclic brGMGTs are known, we also calculated the degree of methylation of 5-methyl brGDGTs without cyclopentane moieties for comparison:.

$$\text{MBT'}_{5\text{me,acyclic}} = \text{Ia}/(\text{Ia} + \text{IIa} + \text{IIIa}) \quad (3)$$

An empirical proxy, that correlated the distribution of specific brGMGT isomers with temperature in a suite of African lake sediments, was calculated following Baxter et al. (2019):.

$$\text{brGMGTI} = (\text{H1020c} + \text{H1034a} + \text{H1034c})/(\text{H1020b} + \text{H1020c} + \text{H1034a} + \text{H1034c} + \text{H1048}) \quad (4)$$

Temperature was estimated using the two temperature models of Baxter et al. (2019) developed for East African lake sediments, based either on the linear correlation between brGMGTI and temperature (R^2 = 0.94, Root Mean Square Error (RMSE) = 2.16 °C):.

$$\text{Temperature } [^\circ\text{C}] = 2.86 + 26.5 \times \text{brGMGTI} \quad (5)$$

Or using the stepwise forward selection (SFS) of the sequentially most abundant brGMGTs in the African lake dataset (R^2 = 0.94, RMSE = 2.20 °C):.

$$\text{Temperature } [^\circ\text{C}] = 1.18 + 0.47 \times \text{H1034a} + 0.12 \times \text{H1020a} + 0.50 \times \text{H1020c} \quad (6)$$

BrGMGT distributions, concentrations, loadings and the calculated proxies were evaluated with (Welch's) ANOVA and (paired) t-tests with R software package for statistical computing (RStudio, v. 1.2.5033; R4.0.4) and SPSS (IBM, v. 26.0.0.0). The level of significance was $p \leq 0.05$. Mean ± standard error (SE) was reported. Concentrations refer to total brGMGT concentrations and not to individual isomers. Spatial patterns were investigated with ArcGIS software (ESRI, v. 10.8.1).

3. Results and discussion

3.1. Occurrence and distribution of brGMGTs in the terrestrial realm: Godavari basin

BrGMGTs with *m/z* 1020 are present in quantifiable amounts in 62% of the terrestrial samples collected in the Godavari basin, with H1020c as generally most abundant compound (fractional abundance: 0.52 ± 0.01 (mean ± standard error)) (Fig. 1b and 3a) (Kirkels et al., 2021a). H1020 isomers occur in 50% of both bulk and fine fraction soils, in 67% and 50% of surface river SPM in the dry and wet season respectively, and in 78% of the subsurface SPM samples in the wet season. H1020 brGMGTs were also detected in 65% and 62% of the bulk riverbed sediments in the dry and wet season respectively, and in 96% of the fine fractions collected in the wet season. Notably, terrestrial Godavari samples that lack H1020 isomers also lack all other brGMGTs. BrGMGTs with *m/z* 1034 were present in 41% of the terrestrial samples, in bulk and fine fraction soils (24% and 10%, respectively) and mainly in wet season SPM (100%) and in bulk dry season riverbed sediments (46%), as well as in bulk (46%) and fine (84%) wet season riverbed sediments. H1034b is the most abundant isomer (fractional abundance: 0.17 ± 0.01), whereas H1034a and H1034c appear in 14% and 13% of all terrestrial Godavari basin samples (fractional abundance: ≤ 0.11). BrGMGTs with *m/z* 1048 were consistently below the detection limit for all Godavari samples.

Comparing the distribution of brGMGTs among the different sample types in the Godavari basin reveals significant differences in the fractional abundances of H1020 isomers ($p \leq 0.01$), while such differences are not found for H1034 isomers (Fig. 3a). Specifically, soils are

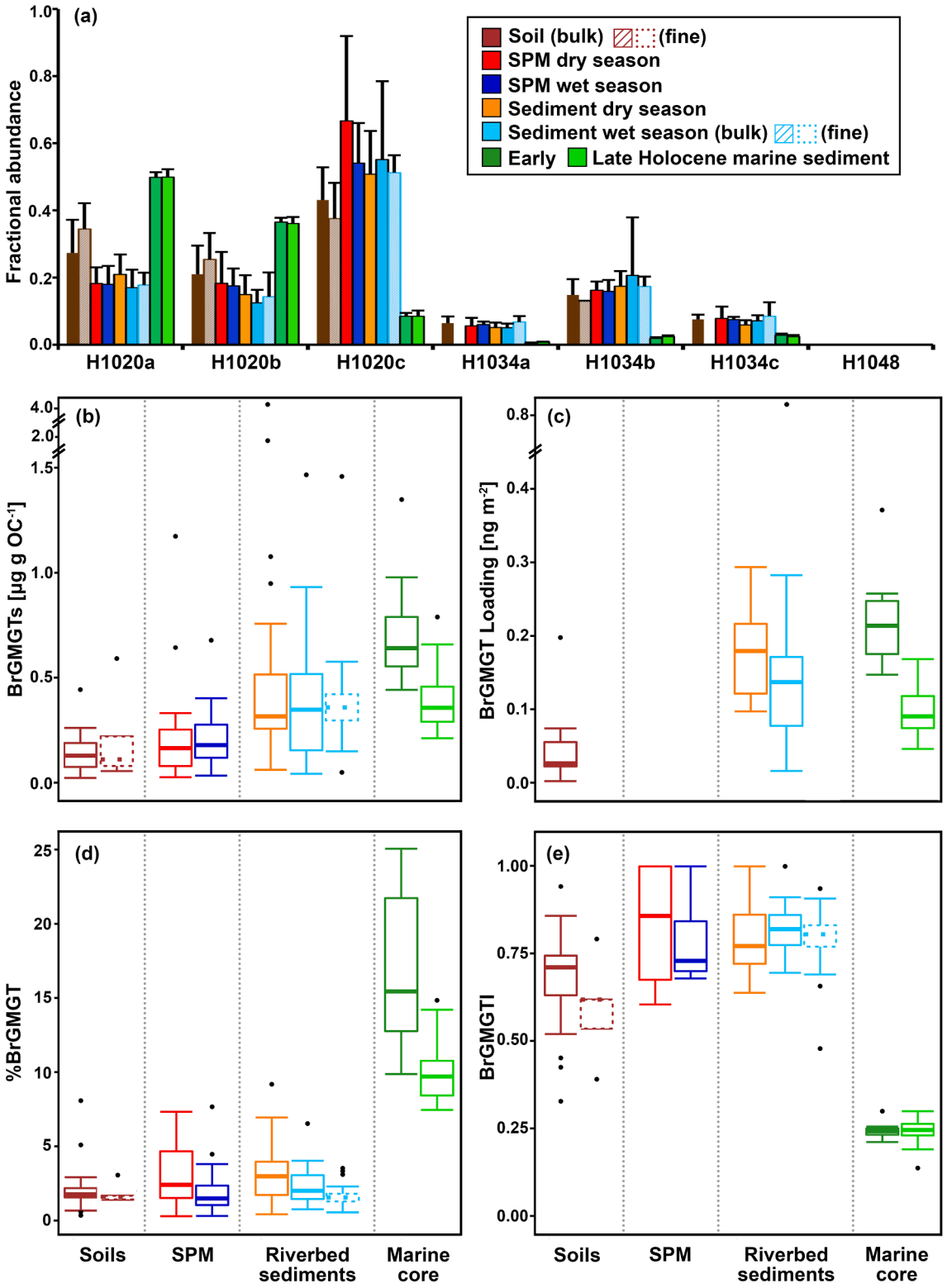

Fig. 3. (a) Average fractional abundances of brGMGTs in (bulk and fine) soils, SPM and (bulk and fine) riverbed sediments collected in the dry and wet season, and in Early and Late Holocene marine sediments retrieved from the Bay of Bengal. The error bars represent the standard deviation. The fine fraction soils and sediments (≤63 µm) are striped. Box-and-whisker plot of (b) BrGMGT concentration normalised to total organic carbon, (c) BrGMGT loadings normalised to mineral surface area (MSA; soil, dry season and Holocene sediment data from Usman et al., 2018), (d) %BrGMGT (i.e., brGMGTs relative to brGDGTs) and (e) BrGMGTI for soils, SPM and riverbed sediments collected in the dry and wet season and for Early and Late Holocene marine sediments. The box represents the first (Q1) and third (Q3) quartiles, and the line in the box represents the median value, the whiskers extent to 1.5×(Q3–Q1) values and outliers are shown as points. Solid lines represent bulk data, dashed lines the fine fractions (≤63 µm).

characterized by (significantly) lower fractional abundances of brGMGT H1020c than SPM and riverbed sediments ($p \leq 0.01$ to $p = 0.28$; Fig. 3a). Accordingly, the fractional abundances of brGMGT H1020a and H1020b are (significantly) higher in soils than in SPM and riverbed sediments (H1020a: $p \leq 0.01$ to $p = 0.14$; H1020b: $p \leq 0.01$ to $p = 0.10$ for sediments and $p > 0.60$ for SPM, respectively; Fig. 3a). Also, the OC-normalised brGMGT concentration changes significantly between sample types ($p \leq 0.01$), where the average brGMGT concentration in Godavari soils is 1.5–1.9 times lower than in SPM and 2.7–4.4 times lower than in riverbed sediments (Fig. 3b).

The absence of all brGMGTs in 50% of all Godavari soils resembles their representation in soils surrounding Lake Chala in East Africa, the only other set of mineral soils studied so far. There, minor amounts of brGMGTs were detected in only four out of seven soils (Baxter et al., 2021). This similarity indicates that brGMGTs are not as ubiquitous in mineral soils, opposed to their abundant occurrence in water-saturated peats and coastal wetlands (Naafs et al., 2018; Lü et al., 2019; Tang et al., 2021). BrGMGT distributions and concentrations are markedly different between soils, SPM and riverbed sediments in the Godavari basin, potentially indicating different brGMGT sources in soils and in the river.

In Lake Chala, the discrepancies in brGMGT distributions and concentrations between soils, SPM, and lake sediments were interpreted as evidence for a primarily in situ source of brGMGTs in the lake sediments (Baxter et al., 2021). Extrapolating these findings to the Godavari basin suggests that brGMGTs in the river may also be produced in situ, although the location of brGMGT production in the river, i.e., water column and/or riverbed sediments, is yet unidentified. Given that brGMGTs occur infrequently in mineral soils, but are abundant in peat and wetland soils points towards an anoxic niche for brGMGT production in soils. Indeed, the Godavari soils in which brGMGTs are detected are regularly irrigated or inundated due to their near-river position and/or fertilized as indicated by their relatively high TN levels (mainly $\geq$ 0.07% versus $\leq$ 0.07% in the majority of soils where brGMGTs are absent; Kirkels et al., 2021a). Similarly, SPM and riverbed sediments in which brGMGTs are present are mainly derived from sites with standing water (e.g., at dams, Reservoir Lake) or near disturbances (agriculture, washing, sewage) where nutrient inputs are likely increased (Balakrishna and Probst, 2005; Pradhan et al., 2014) (Fig. 2b).

The eutrophic setting and quiescent waters behind dams likely facilitated phytoplankton blooms that result in oxygen-limited conditions upon their degradation by bacteria (dissolved oxygen $\leq$ 5 mg/L; Cardoso et al., 2001; CWC, 2009). These conditions mainly occur in the dry season as well as in the upper part of the basin in the wet season, where rainfall was very limited in the year of sampling (Kirkels et al., 2020b). The stagnant conditions resulting from this limited rainfall may have favoured in situ production of brGMGTs at these sites, similar to the observed preferential production of brGMGTs in the anoxic part of the water column and sediments of Lake Chala (Baxter et al., 2021), as well as in the anoxic, water saturated part of peats (Naafs et al., 2018). However, the presumed causal relation between eutrophication and oxygen limitation via algal blooms in the Godavari basin makes it difficult to disentangle and quantify the impact of nutrient and oxygen levels separately on brGMGT production, for which controlled study conditions are necessary.

Furthermore, brGMGTs are ubiquitous in SPM and sediments in the Godavari delta (Fig. 2c). BrGMGTs are particularly prevalent in the Reservoir Lake, where water is standing and nutrients from the upstream basin accumulate, likely facilitating in situ production. As a consequence, brGMGTs are also abundant just downstream of the dam in the wet season when the dam is opened and reservoir-derived material flushes out, as well as in the estuary and near the outflow of the other two branches into the Bay of Bengal following patterns of seawater intrusion (Kirkels et al., 2020b). In the dry season, brGMGTs are also abundant further upstream as seawater reaches further inland due to the low river outflow (Kirkels et al., 2020b). The prevalence of brGMGTs in the estuary and at the fresh/seawater transition may be explained by enhanced degradation of young and labile terrestrial-derived OC in this mixing zone that has been shown to create oxygen-limited conditions/hypoxia (Hou et al., 2021).

Taken together, the occurrence of brGMGTs at sites with relatively high TN and/or low oxygen levels supports the idea that they are produced by anaerobic planktonic microbes involved in N cycling in oxygen-deprived conditions as proposed by Xie et al. (2014). Notably, the brGMGTs in soils and in wet season SPM from the North Tributaries (Penganga/Wardha/Pranhita Rivers; sites: 34–37, 42–43; Fig. 2b) may be linked to the open coal pits in this region, and the finding that brGMGTs are abundant in lignites (Naafs et al., 2018; Inglis et al., 2019). Accordingly, the ^{14}C age of soil OC in the source area of this SPM is consistent with relatively old OC (Usman et al., 2018).

In-river production of brGMGTs in the Godavari River, rather than soils being a major source, is further supported by an increase in OC-normalised brGMGT concentrations from soils (0.1 ± 0.0 μg g^{-1} OC) to SPM collected in the dry (0.3 ± 0.1) and wet (0.2 ± 0.0) season and to riverbed sediments (dry: 0.6 ± 0.2; wet: 0.4 ± 0.1) (Fig. 3b). The latter would support potential production/accumulation in riverbed sediments. Indeed, the average elemental OC/N ratio in riverbed sediments across the Godavari basin (except the delta with complex biogeochemical cycles) in the dry season (7.7 ± 0.7, $n = 23$; data not shown) is in the typical range of riverine phytoplankton-produced organic matter (1–8; Balakrishna and Probst, 2005), but significantly lower than in the Godavari soils (14.2 ± 0.6, $n = 46$; $p \leq 0.001$). In addition, brGMGT loadings on mineral surfaces increase from bulk soils (0.06 ± 0.01 ng m^{-2}) to dry (0.18 ± 0.02; $p \leq 0.001$) and wet (0.20 ± 0.07) season sediments (Fig. 3c, Supplementary Fig. S1), where a downstream decrease would be expected based on the gradual loss or degradation of soil-derived compounds that generally occurs during fluvial transport (Freymond et al., 2018b). Instead, the fact that brGMGT concentrations and their composition are similar for bulk and fine sediments in the wet season ($p > 0.05$; Fig. 3a,b,d), suggests that no preferential loss, transfer or sorting of certain brGMGTs takes place during fluvial transport.

Similarly, SPM collected along river depth profiles in the main stem Middle Godavari (site 28) and in the delta (site 10) in the wet season (Fig. 2b,c), reveal no clear trends in brGMGT concentration, composition or indices with depth (Supplementary Fig. S2), indicating that brGMGTs are well-mixed within the water column without hydrodynamic sorting effects and/or selective transport/production at certain depths, although brGMGTs approximate the detection limit close to the coarse-grained riverbed near the non-eroding bank.

The brGMGT assemblage in the Godavari basin is dominated by four compounds, namely the H1020 isomers and H1034b, which generally appear in the order H1020c > H1020a > H1020b ≈ H1034b (if present) (fractional abundance: 0.52 ± 0.01, 0.21 ± 0.01, 0.17 ± 0.01, 0.17 ± 0.01, respectively) (Fig. 3a and 4). Except for a few agricultural/disturbed bulk ($n = 4$, site 5, 30, 34, 49) and fine fraction ($n = 2$, site 32, 54) soils where H1020a or H1020b dominate, and for a few SPM and sediment samples in the delta ($n = 7$) and basin (site 25, 42, 47) where only H1020c is above the detection limit at very low brGMGT concentrations (mainly ≤ 0.1 μg g^{-1} OC) (Fig. 2b and 4). The general brGMGT distribution and the predominance of H1020c in the Godavari basin, where the average MAAT is ~ 27 °C, is in line with the brGMGT distributions in sediments from East African lakes with MAAT > 20 °C, whereas brGMGT distributions in African lake sediments with MAAT < 12 °C) and in the cold mid-Paleocene part of the Pacific Ocean record are all characterised by low contributions of H1020c (Baxter et al., 2019; Bijl et al., 2021), supporting the presumed temperature control on the biosynthesis of brGMGTs.

The predominance of brGMGT H1020 isomers in the Godavari basin results in an H-MBT index close to 1, with values ranging between 0.79 ± 0.04 in wet season riverbed sediments and 0.97 ± 0.03 in fine fraction soils. These high H-MBT values resemble those of the MBT'_{5me} (and $MBT'_{5me,acyclic}$) index for Godavari soils that approximate 1.0 due to the

predominance of brGDGT Ia in these soils (Dearing Crampton-Flood et al., 2019, 2020). The near-saturation of the brGMGT-based H-MBT and brGDGT-based MBT'$_{5me(/acyclic)}$ indices in Godavari soils suggests that both indices lose their sensitivity to temperature change at temperatures > 25 °C. The comparable behaviour of H-MBT and MBT'$_{5me(/acyclic)}$ in the Godavari basin furthermore suggests that the degree of methylation of brGMGTs and brGDGTs responds to MAAT in a similar manner, as has been found in peats (Naafs et al., 2018). BrGMGTI, an empirical proxy that strongly correlated with MAAT in African Lake sediments (Baxter et al., 2019), roughly approaches 1 (0.80 ± 0.01, n = 110) in SPM and sediments in the Godavari basin (Fig. 3e) which is within the same range as lakes with MAAT > 20 °C, supporting a temperature control on brGMGT distributions.

In addition, the %brGMGT has been shown to increase with higher ambient or water temperatures in tropical peats and lakes (Naafs et al., 2018; Baxter et al., 2019). In the Godavari basin, %brGMGT varies between 0.3% and 9.2% (2.3 ± 0.1%; n = 138, where both brGMGTs and brGDGTs are present) in soils, SPM and sediments without a clear spatial or seasonal trend (Fig. 3d), indicating no preferential production/preservation of brGMGTs relative to brGDGTs. The %brGMGT values for the Godavari basin are in the same range as those for Lake Chala's SPM and soils with a comparable MAAT (0.1–8.4, 2.4 ± 0.1%, n = 166; MAAT: 25 °C; Baxter et al., 2021), but at the lower end of the range in % brGMGT observed in a global compilation of modern peats (1.8–19.9, 7.4 ± 0.4%, n = 109; Naafs et al., 2018) and East African lake sediments (4.2–30.9, 14.3 ± 1.2%, n = 32; Baxter et al., 2019) with MAATs (>20 °C). However, a recent study of brGMGTs in and around Lake Chala revealed that lake sediments have a higher %brGMGT (9.1–12.5, 10.7 ± 1.0%, n = 3) than soils and SPM due to additional production of brGMGTs in the anoxic sediment layer (Baxter et al., 2021).

Taken together, the similar response of brGMGTs and brGDGTs to temperature and consistent behaviour of %brGMGT at relatively uniform MAATs across the Godavari basin, supports the hypothesis that in the terrestrial realm both may be produced by the same group of organisms (Naafs et al., 2018), presumably Acidobacteria (Sinninghe Damsté et al., 2018; Halamka et al., 2021).

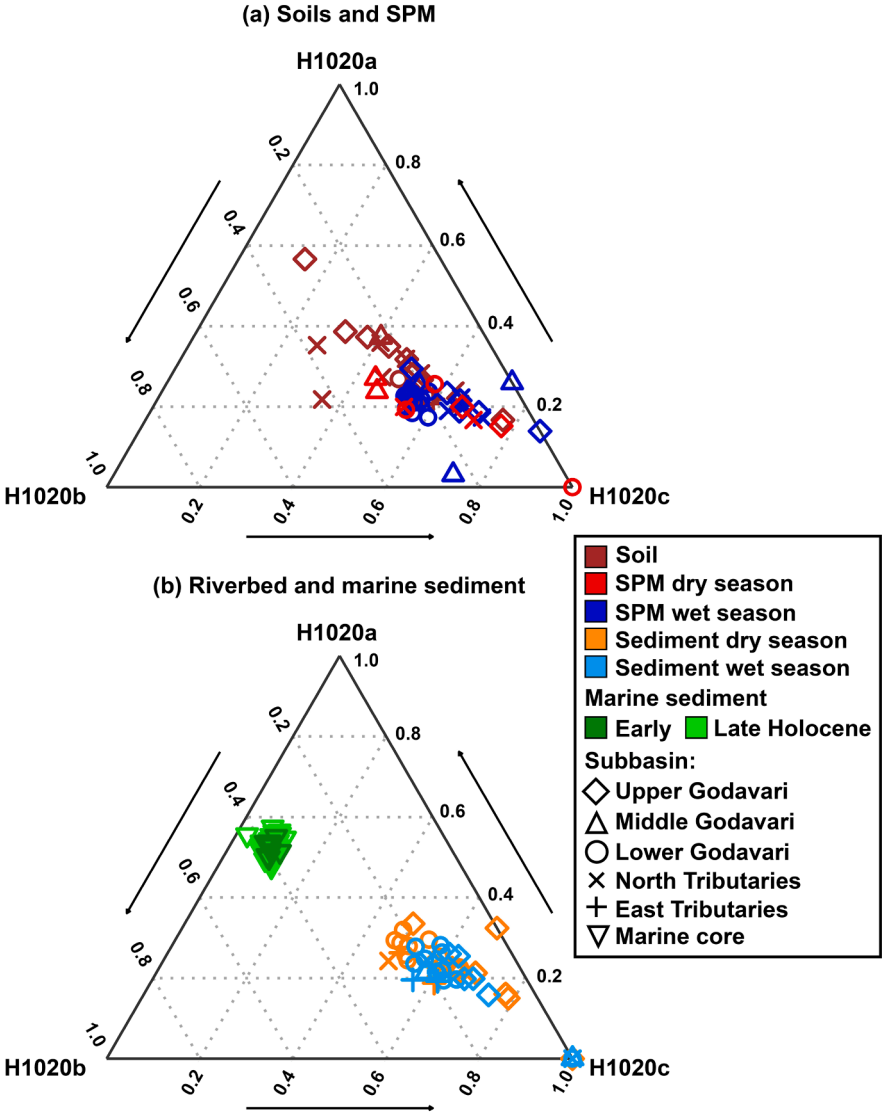

Fig. 4. Proportions of the major brGMGTs H1020a, H1020b and H1020c for (a) soils and SPM and (b) riverbed sediments collected in the dry and wet season and Early and Late Holocene marine sediments from the Bay of Bengal. The symbols represent the different subbasins, only bulk soils and riverbed sediments are presented (their composition is similar to the fine fractions).

3.2. Occurrence and distribution of brGMGTs in the marine realm: Bay of Bengal sediments

Marine sediments deposited in the Bay of Bengal over the Holocene period have a continuous presence of all brGMGTs isomers with *m/z* 1020 and 1034, but no detectable amounts of H1048 (Figs. 1c and 3a) (Kirkels et al., 2021b). BrGMGT concentrations are 0.2 to 1.3 μg g^{-1} OC (0.5 ± 0.0, n = 46) and generally higher than in the Godavari basin samples (p = 0.07) (Fig. 3b). The %brGMGT is 7.5–25.1 (11.5 ± 0.6), which is significantly higher than in the modern basin ($p \leq 0.001$) (Fig. 3d). Also, the composition of brGMGTs in the Bay of Bengal sediments is significantly different from that in the basin and is characterised by H1020a > H1020b > H1020c > H1034c ≈ H1034b > H1034a (fractional abundance: 0.50, 0.36, 0.08, 0.02, 0.02, 0.01 (all ± 0.00), respectively; $p \leq 0.001$) (Fig. 3a).

Interestingly, the distribution of the H1020 isomers (i.e., most dominant brGMGTs) gradually changes along the Godavari River. The H1020c that is dominant in SPM and riverbed sediments in the Upper Godavari decreases towards and in the delta, coinciding with an increase in H1020a (Fig. 4a,b). This trend is most pronounced in the dry season, when the delta experiences seawater intrusion, whereas the river plume extends beyond the mouth in the wet season (Sridhar et al., 2008; Kirkels et al., 2020b), and hints towards a contribution of brGMGTs with a marine origin at the river-sea transition, mostly of H1020a and H1020b that also dominate the marine sediment core (Fig. 4). The compositional shift in brGMGTs from land to sea and the marked increase in %brGMGT in the marine sediment core suggest that these brGMGTs are more likely produced in the marine environment rather than received from the terrestrial realm.

The negligible transfer from soil to sea is further supported by the fact that brGMGT loadings on mineral surfaces are on average ~ 2 times higher in the Bay of Bengal than in (bulk) soils in the Godavari basin (0.13 ± 0.01 vs 0.06 ± 0.01 ng m^{-2}; $p \leq 0.001$) (Fig. 3c, Supplementary Fig. S1), suggesting likely brGMGT addition by marine production. In contrast, the loadings of *n*-alkanoic acids with a known terrestrial origin remained in the same range along the same continuum (Usman et al., 2018). Our findings thus confirm a predominant marine source of brGMGTs in marine sediments, as was previously assumed for Eocene Arctic and Paleocene southwest Pacific Ocean sediments (Sluijs et al., 2020; Bijl et al., 2021).

Although the exact producers of brGMGTs remain elusive, Sluijs et al. (2020) suggested that an increase in %brGMGT across the warm Eocene period could represent marine production related to a drop in seawater oxygen levels following warming and sea level rise, which would be in line with their production by anaerobic microbes (Xie et al., 2014).

The %brGMGT in the Bay of Bengal core shows a shift toward lower values from 16.7 ± 1.6 (n = 11) to 9.8 ± 0.3% (n = 35) ($p \leq 0.01$) at the transition from the Early to Late Holocene at ~ 4700 yr BP (Fig. 5a). However, the %brGMGT record does not match sea surface temperatures (SSTs), which remain high and vary within a small range (27–29.5 °C; Govil and Naidu, 2011) in the Bay of Bengal over the Holocene period (Fig. 5b). The H-MBT index is again very close to 1.0 (approaching 'saturation') due to the predominance of H1020 isomers (Fig. 5c). In contrast, brGMGTI is 0.24 ± 0.01 (range: 0.14–0.30) across the Holocene (Fig. 5d) and values are mainly driven by the predominance of H1020b in the sediment core. BrGMGTI values in the Bay of Bengal core are significantly lower than in the Godavari basin ($p \leq 0.001$) (Fig. 3e), and much lower than in East African lake sediments (0.76 ± 0.01, n = 23, range: 0.61–0.87) with comparable surface water temperatures > 25 °C (Baxter et al., 2019).

Contrary to Bijl et al. (2021), there is no correlation found between SST and brGMGTI values for the Bay of Bengal sediments (Fig. 5b,d). The average brGMGT-inferred estimates of temperature in the Bay of Bengal core using the brGMGTI and SFS models of Baxter et al. (2019) are 9.3 °C and 11.7 °C, respectively (Fig. 5e). These temperature estimates approximate the bottom water temperature of ~8 °C at 1250 m depth where the core was taken, which was determined based on linear interpolation of measured water temperatures of ~9.5 °C at 500 m (Murty et al., 1992) and ~5 °C at 3000 m depth (Shetye et al., 1996) in the western part of the Bay of Bengal.

The exact sites of brGMGT production in the marine realm are as yet unidentified, but the brGMGT-inferred temperature estimates for the Bay of Bengal core resemble bottom water rather than surface water temperatures and this may be speculatively interpreted as brGMGT production deep in the water column or in marine sediments rather than in surface waters. The limited downcore variation in the isomeric composition of brGMGTs and in brGMGT-based indices (i.e., H-MBT and brGMGTI) (Fig. 4b, 5c,d) would be consistent with brGMGT production at a relatively constant bottom water temperature (Shetye et al., 1996).

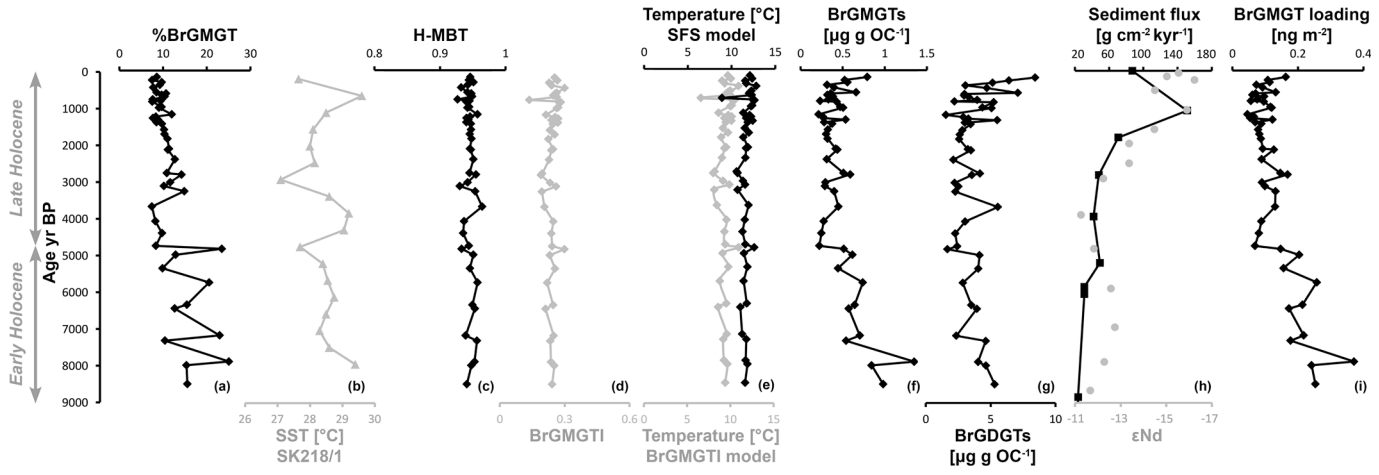

Fig. 5. BrGMGT proxies and sediment properties of Holocene marine core NGHP-01-16A (this study: diamond), retrieved ~40 km from the Godavari mouth in the Bay of Bengal and sea surface temperatures for the western Bay of Bengal (core SK218/1; triangle) for the same time interval. The age model from Usman et al. (2018) is used for core NGHP-01-16A. (a) %BrGMGT, (b) sea surface temperature (SST) based on Mg/Ca in foraminifera from core SK218/1 (data from Govil and Naidu, 2011), (c) H-MBT, (d) BrGMGTI, (e) Reconstructed temperature based on brGMGTI and SFS models of Baxter et al. (2019), (f) BrGMGT concentration normalised to total organic carbon, (g) BrGDGT concentration normalised to total organic carbon (data from Kirkels et al., 2021d), (h) Sediment flux (square) and εNd isotopic signatures (circle) (εNd end-members: –1 ± 5 for flood basalts in the Deccan Plateau (i.e., upper basin) and –35 ± 8 for felsic bedrocks in the lower basin) (data from Giosan et al., 2017), and (i) BrGMGT loading normalised to mineral surface area (MSA, data from Usman et al., 2018).

However, knowledge on brGMGT distributions in the marine realm is still very limited, including alternative scenarios that marine brGMGTs may be influenced by other factors than temperature or may have a different temperature relation than in the terrestrial realm. Our findings on the Bay of Bengal core together with contrasting findings for the two marine brGMGT paleorecords (Sluijs et al., 2020; Bijl et al., 2021) underline the importance of further research on brGMGTs in the marine realm and on the applicability of calibration models to determine marine brGMGT–temperature relations.

In the Bay of Bengal core, the shift in %brGMGT is mainly the result of decreasing brGMGT concentrations from the Early (0.7 ± 0.1 μg g^{-1} OC) to the Late Holocene (0.4 ± 0.0 μg g^{-1} OC; $p \leq 0.01$) and (slightly) increasing brGDGT concentrations (Fig. 5a,f,g). Notably, the timing of the shift in %brGMGT corresponds with an increase in the sediment load exported from the Upper Godavari to the Bay of Bengal inferred from changes in sedimentological and biomarker signatures (Fig. 5h), and coincides with major climatic and anthropogenic changes in the Godavari basin (Ponton et al., 2012; Giosan et al., 2017; Usman et al., 2018). For example, Ponton et al. (2012) and Cui et al. (2017) reported on aridification associated with a change from C3 to aridity-adapted C4 vegetation and reduced vegetation coverage from the Early to Late Holocene in the Godavari basin. Simultaneously, expansion of agriculture and population growth were indicated by findings at archaeological sites (e.g., Ponton et al., 2012; Cui et al., 2017). Taken together, these changes resulted in increased soil erosion, predominantly from the Deccan plateau in the upper Godavari basin, and higher sedimentation rates in the Bay of Bengal (Giosan et al., 2017; Usman et al., 2018). Hence, the shift in %brGMGT may be related to increased export to the Bay of Bengal of terrestrial-derived material that is relatively depleted in brGMGTs, changing depositional conditions with rapid burial and potentially efficient preservation of this terrestrial material and/or reduced production of brGMGTs in the marine realm. The first is consistent with the simultaneous shift toward lower brGMGT loadings from 0.22 ± 0.02 in the Early to 0.10 ± 0.01 ng m^{-2} in the Late Holocene ($p \leq 0.001$), as they are also low in the Godavari basin soils (Fig. 3c and 5i).

The high sedimentation rates observed over the Late Holocene (Giosan et al., 2017) may speculatively hinder brGMGT production in the deeper water column or sediment layer. Alternatively, the decrease in %brGMGT may be explained by preferential degradation of brGMGTs over brGDGTs, although it is difficult to ascertain a driving mechanism. Although the C–C bond of the brGMGTs is presumed to enhance membrane stability, preferential degradation is unlikely given that the ether bonds contained in both brGMGTs and brGDGTs are first attacked during degradation (Liu et al., 2016; Naafs et al., 2018). In addition, both brGDGTs and brGMGTs appear to be well preserved in sedimentary archives as old as the Paleocene (Bijl et al., 2021).

So far, an influence of pH on brGMGTs has been studied empirically for terrestrial samples, including in peats (Naafs et al., 2018) and lakes (Baxter et al., 2019, 2021), and no correlation was found in either setting, although Tang et al. (2021) suggested that pH may exert an influence on the occurrence of brGMGTs in peat archives at lower temperatures. However, the absence of a pH change between the Godavari basin (~8; Dearing Crampton-Flood et al., 2020) and the Bay of Bengal (~8.1; Sarma et al., 2015), provides no additional clues on pH effects on brGMGTs in our marine record.

The differences in brGMGT signals in the Bay of Bengal core and the modern Godavari basin, as well as in modern and ancient peats (Naafs et al., 2018; Tang et al., 2021), lacustrine (Baxter et al., 2019, 2021) and Paleocene Arctic and Pacific Ocean sediments (Sluijs et al., 2020; Bijl et al., 2021) demonstrate that more research is needed on brGMGT producers, their sourcing and environmental dependencies, to further assess their proxy potential for paleoreconstructions.

4. Conclusions

Our assessment of the occurrence and distribution of brGMGTs along a soil-river-sea continuum from the modern Godavari basin to Holocene marine sediments in the Bay of Bengal reveals that H1020 isomers dominate, with limited contribution by H1034 isomers and no detectable amounts of H1048. In the terrestrial realm, brGMGTs are generally present at sites that are characterised by high nutrient levels and/or oxygen-limited conditions, suggesting anaerobic microbes involved in N cycling as likely source. In the marine realm, H1020 and H1034 isomers occur continuously in the Bay of Bengal sediment core, but with a different isomeric composition than in the modern basin, indicating a primarily marine source, rather than transfer/preservation of the terrestrial-derived brGMGTs. Downcore changes in %brGMGT do not track temperature, but appear instead to be linked to an increase in terrestrial input at the transition from the Early to Late Holocene, coinciding with major changes in sediment sourcing and aridification of the basin. The limited variation in brGMGT composition and brGMGT-based indices such as H-MBT and brGMGTI downcore, combined with brGMGT-inferred temperature estimates which resemble bottom water temperature, may be interpreted as brGMGT production in the deep water column and/or in sediments in the marine realm. However, further research on brGMGTs is needed to identify their exact producers, as well as the environmental/climatological signal they carry to establish the value of brGMGT-based proxies in paleoclimate reconstructions.

Declaration of Competing Interest

The authors declare that they have no known competing financial interests or personal relationships that could have appeared to influence the work reported in this paper.

Acknowledgements

This research was supported by Veni Grant 863.13.016 from the Netherlands Organisation for Scientific Research (NWO) to F.P. at Utrecht University (UU). We are grateful to Prof. Prasanta Sanyal from the Indian Institute of Science Education and Research (IISER) in Kolkata (India) for his help to organise the fieldwork in the Godavari basin. We thank Dr. Maarten Lupker (ETH Zurich), Dr. Sayak Basu (IISER), Chris Martes (UU) and Huub Zwart (UU) for their assistance in the field. We further thank Prof. Liviu Giosan and Dr. Camilo Ponton (Woods Hole Oceanographic Institute) for access to the Bay of Bengal core and Suning Hou (UU), Dr. Klaas Nierop (UU), Dr. Ellen Hopmans (NIOZ) and Dr. Marcel van der Meer (NIOZ) for laboratory assistance. We thank Yan Bai and two anonymous reviewers for constructive feedback that greatly improved the manuscript.

Data availability

Data from this paper are available in the *Pangaea* database. BrGMGT and geochemical data for the Godavari basin (Kirkels et al., 2021a; https://doi.org/10.1594/PANGAEA.937965) and Bay of Bengal core (Kirkels et al., 2021b; https://doi.org/10.1594/PANGAEA.937932). BrGDGT and geochemical data for the Godavari basin (Kirkels et al., 2021c; https://doi.org/10.1594/PANGAEA.934712) and the Bay of Bengal core (Kirkels et al., 2021d; https://doi.org/10.1594/PANGAEA.934701). BrGDGT data for the Godavari soils are included in the global soil and peat branched GDGT compilation dataset by Dearing Crampton-Flood et al. (2019) (https://doi.org/10.1016/j.gca.2019.09.043).

Appendix A. Supplementary material

Supplementary data to this article can be found online at https://doi.org/10.1016/j.orggeochem.2022.104405.

References

Babar, M., Kaplay, R.D., 2018. Godavari River: geomorphology and socio-economic characteristics. In: Singh, D.S. (Ed.), The Indian Rivers. Springer, Singapore, pp. 319–337.

Balakrishna, K., Probst, J.L., 2005. Organic carbon transport and C/N ratio variations in a large tropical river: Godavari as a case study, India. Biogeochemistry 73, 457–473.

Baxter, A.J., Hopmans, E.C., Russell, J.M., Sinninghe Damsté, J.S., 2019. Bacterial GMGTs in East African lake sediments: their potential as palaeotemperature indicators. Geochimica et Cosmochimica Acta 259, 155–169.

Baxter, A.J., Peterse, F., Verschuren, D., Sinninghe Damsté, J.S., 2021. Anoxic *in situ* production of bacterial GMGTs in the water column and surficial bottom sediments of a meromictic tropical crater lake: implications for lake paleothermometry. Geochimica et Cosmochimica Acta 306, 171–188.

Bianchi, T.S., Cui, X., Blair, N.E., Burdige, D.J., Eglinton, T.I., Galy, V., 2018. Centers of organic carbon burial and oxidation at the land-ocean interface. Organic Geochemistry 115, 138–155.

Bijl, P.K., Frieling, J., Cramwinckel, M.J., Boschman, C., Sluijs, A., Peterse, F., 2021. Maastrichtian-Rupelian paleoclimates in the southwest Pacific–a critical evaluation of biomarker paleothermometry and dinoflagellate cyst paleoecology at ocean drilling program site 1172. Climate of the Past 17, 2393–2425.

Biksham, G., Subramanian, V., 1988a. Nature of solute transport in the Godavari basin, India. Journal of Hydrology 103, 375–392.

Biksham, G., Subramanian, V., 1988b. Sediment transport of the Godavari River basin and its controlling factors. Journal of Hydrology 101 (1-4), 275–290.

Cardoso, A.C., Duchemin, J., Magoarou, P., Premazzi, G., 2001. Criteria for the identification of freshwaters subject to eutrophication; their use for the implementation of the "nitrates" and urban waste water directives. European Commission - Joint Research Centre. Office for official publications of the European communities, Luxembourgh, pp. 1–87. https://op.europa.eu/en/publication-detail/-/publication/26a9c3bb-a4c2-11e7-837e-01aa75ed71a1.

Cui, M., Wang, Z., Nageswara Rao, K., Sangode, S.J., Saito, Y., Chen, T., Kulkarni, Y.R., Naga Kumar, K.C.V., Demudu, G., 2017. A mid-to late-Holocene record of vegetation decline and erosion triggered by monsoon weakening and human adaptations in the south-east Indian Peninsula. The Holocene 27, 1976–1987.

CWC (Central Water Commission), 2009. Integrated Hydrological Databook. Government of India, Ministry of Water Resources. New Delhi, pp. 1–381. https://www.indiawaterportal.org/articles/integrated-hydrological-and-water-data-books-central-water-commission-2005-09.

Dearing Crampton-Flood, E., Peterse, F., Munsterman, D., Sinninghe Damsté, J.S., 2018. Using tetraether lipids archived in North Sea Basin sediments to extract North Western European Pliocene continental air temperatures. Earth and Planetary Science Letters 490, 193–205.

Dearing Crampton-Flood E., Tierney J.E., Peterse F., Kirkels, Frédérique M.S.A., Sinninghe Damsté J.S., 2019. Global soil and peat branched GDGT compilation dataset. PANGAEA, https://doi.org/10.1016/j.gca.2019.09.043.

Dearing Crampton-Flood, E., Tierney, J.E., Peterse, F., Kirkels, F.M.S.A., Sinninghe Damsté, J.S., 2020. BayMBT: A Bayesian calibration model for branched glycerol dialkyl glycerol tetraethers in soils and peats. Geochimica et Cosmochimica Acta 268, 142–159.

De Jonge, C., Hopmans, E.C., Stadnitskaia, A., Rijpstra, W.I.C., Hofland, R., Tegelaar, E., Sinninghe Damsté, J.S., 2013. Identification of novel penta-and hexamethylated branched glycerol dialkyl glycerol tetraethers in peat using HPLC–MS^2, GC–MS and GC–SMB-MS. Organic Geochemistry 54, 78–82.

De Jonge, C., Hopmans, E.C., Zell, C.I., Kim, J.-H., Schouten, S., Sinninghe Damsté, J.S., 2014a. Occurrence and abundance of 6-methyl branched glycerol dialkyl glycerol tetraethers in soils: implications for palaeoclimate reconstruction. Geochimica et Cosmochimica Acta 141, 97–112.

De Jonge, C., Stadnitskaia, A., Hopmans, E.C., Cherkashov, G., Fedotov, A., Sinninghe Damsté, J.S., 2014b. In situ produced branched glycerol dialkyl glycerol tetraethers in suspended particulate matter from the Yenisei River, Eastern Siberia. Geochimica et Cosmochimica Acta 125, 476–491.

Dubois, N., Oppo, D.W., Galy, V.V., Mohtadi, M., van der Kaars, S., Tierney, J.E., Rosenthal, Y., Eglinton, T.I., Lückge, A., Linsley, B.K., 2014. Indonesian vegetation response to changes in rainfall seasonality over the past 25,000 years. Nature Geoscience 7, 513–517.

Eglinton, T.I., Galy, V.V., Hemingway, J.D., Feng, X., Bao, H., Blattmann, T.M., Dickens, A.F., Gies, H., Giosan, L., Haghipour, N., Hou, P., Lupker, M., McIntyre, C. P., Montluçon, D.B., Peucker-Ehrenbrink, B., Ponton, C., Schefuß, E., Schwab, M.S., Voss, B.M., Wacker, L., Wu, Y., Zhao, M., 2021. Climate control on terrestrial biospheric carbon turnover. Proceedings of the National Academy of Sciences 118. https://doi.org/10.1073/pnas.2011585118.

Freymond, C.V., Lupker, M., Peterse, F., Haghipour, N., Wacker, L., Filip, F., Giosan, L., Eglinton, T.I., 2018a. Constraining instantaneous fluxes and integrated compositions of fluvially discharged organic matter. Geochemistry, Geophysics, Geosystems 19, 2453–2462.

Freymond, C.V., Kündig, N., Stark, C., Peterse, F., Buggle, B., Lupker, M., Plötze, M., Blattmann, T.M., Filip, F., Giosan, L., Eglinton, T.I., 2018b. Evolution of biomolecular loadings along a major river system. Geochimica et Cosmochimica Acta 223, 389–404.

Galy, V., France-Lanord, C., Lartiges, B., 2008. Loading and fate of particulate organic carbon from the Himalaya to the Ganga-Brahmaputra delta. Geochimica et Cosmochimica Acta 72, 1767–1787.

Giosan, L., Ponton, C., Usman, M., Glusztajn, J., Fuller, D.Q., Galy, V., Haghipour, N., Johnson, J.E., McIntyre, C., Wacker, L., 2017. Massive erosion in monsoonal central India linked to late Holocene land cover degradation. Earth Surface Dynamics 5, 781–789.

Goñi, M.A., Yunker, M.B., Macdonald, R.W., Eglinton, T.I., 2000. Distribution and sources of organic biomarkers in arctic sediments from the Mackenzie River and Beaufort Shelf. Marine Chemistry 71, 23–51.

Govil, P., Naidu, P.D., 2011. Variations of Indian monsoon precipitation during the last 32 kyr reflected in the surface hydrography of the Western Bay of Bengal. Quaternary Science Reviews 30, 3871–3879.

Halamka, T.A., McFarlin, J.M., Younkin, A.D., Depoy, J., Dildar, N., Kopf, S.H., 2021. Oxygen limitation can trigger the production of branched GDGTs in culture. Geochemical Perspectives Letters 19, 36–39.

Hopmans, E.C., Schouten, S., Sinninghe Damsté, J.S., 2016. The effect of improved chromatography on GDGT-based palaeoproxies. Organic Geochemistry 93, 1–6.

Hopmans, E.C., Weijers, J.W.H., Schefuß, E., Herfort, L., Sinninghe Damsté, J.S., Schouten, S., 2004. A novel proxy for terrestrial organic matter in sediments based on branched and isoprenoid tetraether lipids. Earth and Planetary Science Letters 224, 107–116.

Hou, P., Yu, M., Zhao, M., Montluçon, D.B., Su, C., Eglinton, T.I., 2020. Terrestrial biomolecular burial efficiencies on continental margins. Journal of Geophysical Research: Biogeosciences 125, 1–15.

Hou, P., Eglinton, T.I., Yu, M., Montluçon, D.B., Haghipour, N., Zhang, H., Jin, G., Zhao, M., 2021. Degradation and aging of terrestrial organic carbon within estuaries: biogeochemical and environmental implications. Environmental Science & Technology 55, 10852–10861.

Huguet, C., Hopmans, E.C., Febo-Ayala, W., Thompson, D.H., Sinninghe Damsté, J.S., Schouten, S., 2006. An improved method to determine the absolute abundance of glycerol dibiphytanyl glycerol tetraether lipids. Organic Geochemistry 37, 1036–1041.

Inglis, G.N., Farnsworth, A., Collinson, M.E., Carmichael, M.J., Naafs, B.D.A., Lunt, D.J., Valdes, P.J., Pancost, R.D., 2019. Terrestrial environmental change across the onset of the PETM and the associated impact on biomarker proxies: a cautionary tale. Global and Planetary Change 181, 1–8.

Keil, R.G., Mayer, L.M., Quay, P.D., Richey, J.E., Hedges, J.I., 1997. Loss of organic matter from riverine particles in deltas. Geochimica et Cosmochimica Acta 61, 1507–1511.

Kirkels, F.M., Ponton, C., Galy, V., West, A.J., Feakins, S.J., Peterse, F., 2020a. From Andes to Amazon: assessing branched tetraether lipids as tracers for soil organic carbon in the Madre de Dios River system. Journal of Geophysical Research: Biogeosciences 125, 1–18.

Kirkels, F.M., Zwart, H.M., Basu, S., Usman, M.O., Peterse, F., 2020b. Seasonal and spatial variability in $\delta^{18}O$ and δD values in waters of the Godavari River basin: insights into hydrological processes. Journal of Hydrology: Regional Studies 30, 1–25.

Kirkels F., Zwart H., Usman, M., Peterse F., 2021a. Branched glycerol monoalkyl glycerol tetraethers (brGMGTs) and geochemical proxies in soils, SPM and riverbed sediments in the Godavari River basin (India). PANGAEA, https://doi.org/10.1594/PANGAEA.937965.

Kirkels F., Usman M., Peterse F., 2021b. Branched glycerol monoalkyl glycerol tetraethers (brGMGTs) in a Holocene sediment core (NGHP-01-16A) in front of the Godavari River in the Bay of Bengal (India). PANGAEA, https://doi.org/10.1594/PANGAEA.937932.

Kirkels F., Zwart H., Usman, M., Peterse F., 2021c. Branched glycerol dialkyl glycerol tetraethers, crenarchaeol and geochemical parameters in soils, SPM and riverbed sediments in the Godavari River basin (India). PANGAEA, https://doi.org/10.1594/PANGAEA.934712.

Kirkels, F., Usman, M., Hou, S., Ponton, C., Peterse, F., 2021d. Glycerol dialkyl glycerol tetraethers in a Holocene sediment core (NGHP-01-16A). in front of the Godavari River in the Bay of Bengal (India). https://doi.org/10.1594/PANGAEA.934701.

Li, Z., Sun, Y., Nie, X., 2020. Biomarkers as a soil organic carbon tracer of sediment: recent advances and challenges. Earth Science Reviews 103277, 1–13.

Liu, X.-L., Summons, R.E., Hinrichs, K.-U., 2012. Extending the known range of glycerol ether lipids in the environment: structural assignments based on tandem mass spectral fragmentation patterns. Rapid Communications in Mass Spectrometry 26, 2295–2302.

Liu, X.-L., Birgel, D., Elling, F.J., Sutton, P.A., Lipp, J.S., Zhu, R., Zhang, C., Könneke, M., Peckmann, J., Rowland, S.J., Summons, R.E., Hinrichs, K.-U., 2016. From ether to acid: a plausible degradation pathway of glycerol dialkyl glycerol tetraethers. Geochimica et Cosmochimica Acta 183, 138–152.

Lü, X., Liu, X., Xu, C., Song, J., Li, X., Yuan, H., Li, N., Wang, D., Yuan, H., Ye, S., 2019. The origins and implications of glycerol ether lipids in China coastal wetland sediments. Scientific Reports 9, 1–11.

Lupker, M., France-Lanord, C., Lavé, J., Bouchez, J., Galy, V., Métivier, F., Gaillardet, J., Lartiges, B., Mugnier, J., 2011. A Rouse-based method to integrate the chemical composition of river sediments: application to the Ganga basin. Journal of Geophysical Research: Earth Surface 116, 1–24.

Morii, H., Eguchi, T., Nishihara, M., Kakinuma, K., König, H., Koga, Y., 1998. A novel ether core lipid with H-shaped C_{80}-isoprenoid hydrocarbon chain from the hyperthermophilic methanogen *Methanothermus fervidus*. Biochimica et Biophysica Acta -Lipids and Lipid Metabolism 1390, 339–345.

Murty, V.S.N., Sarma, Y.V.B., Rao, D.P., Murty, C.S., 1992. Water characteristics, mixing and circulation in the Bay of Bengal during southwest monsoon. Journal of Marine Research 50, 207–228.

Naafs, B.D.A., McCormick, D., Inglis, G.N., Pancost, R.D., 2018. Archaeal and bacterial H-GDGTs are abundant in peat and their relative abundance is positively correlated with temperature. Geochimica et Cosmochimica Acta 227, 156–170.

Pancost, R.D., Boot, C.S., 2004. The palaeoclimatic utility of terrestrial biomarkers in marine sediments. Marine Chemistry 92, 239–261.
Peterse, F., Kim, J.-H., Schouten, S., Kristensen, D.K., Koç, N., Sinninghe Damsté, J.S., 2009. Constraints on the application of the MBT/CBT palaeothermometer at high latitude environments (Svalbard, Norway). Organic Geochemistry 40, 692–699.
Ponton, C., Giosan, L., Eglinton, T.I., Fuller, D.Q., Johnson, J.E., Kumar, P., Collett, T.S., 2012. Holocene aridification of India. Geophysical Research Letters 39. https://doi.org/10.1029/2011GL050722.
Pradhan, U.K., Wu, Y., Shirodkar, P.V., Zhang, J., Zhang, G., 2014. Multi-proxy evidence for compositional change of organic matter in the largest tropical (peninsular) river basin of India. Journal of Hydrology 519, 999–1009.
Sarma, V., Paul, Y.S., Vani, D.G., Murty, V., 2015. Impact of river discharge on the coastal water pH and pCO_2 levels during the Indian Ocean Dipole (IOD) years in the western Bay of Bengal. Continental Shelf Research 107, 132–140.
Schouten, S., Baas, M., Hopmans, E.C., Reysenbach, A.-L., Sinninghe Damsté, J.S., 2008. Tetraether membrane lipids of Candidatus *"Aciduliprofundum boonei"*, a cultivated obligate thermoacidophilic euryarchaeote from deep-sea hydrothermal vents. Extremophiles 12, 119–124.
Schefuß, E., Schouten, S., Schneider, R.R., 2005. Climatic controls on central African hydrology during the past 20,000 years. Nature 437, 1003–1006.
Shetye, S.R., Gouveia, A.D., Shankar, D., Shenoi, S.S.C., Vinayachandran, P.N., Sundar, D., Michael, G.S., Nampoothiri, G., 1996. Hydrography and circulation in the western Bay of Bengal during the northeast monsoon. Journal of Geophysical Research: Oceans 101, 14011–14025.
Singh, P.K., Singh, M.P., Prachiti, P.K., Kalpana, M.S., Manikyamba, C., Lakshminarayana, G., Singh, A.K., Naik, A.S., 2012. Petrographic characteristics and carbon isotopic composition of Permian coal: implications on depositional environment of Sattupalli coalfield, Godavari Valley, India. International Journal of Coal Geology 90-91, 34–42.
Sinninghe Damsté, J.S., Rijpstra, W.I.C., Foesel, B.U., Huber, K.J., Overmann, J., Nakagawa, S., Kim, J.J., Dunfield, P.F., Dedysh, S.N., Villanueva, L., 2018. An overview of the occurrence of ether-and ester-linked *iso*-diabolic acid membrane lipids in microbial cultures of the Acidobacteria: Implications for brGDGT paleoproxies for temperature and pH. Organic Geochemistry 124, 63–76.
Sluijs, A., Frieling, J., Inglis, G.N., Nierop, K.G.J., Peterse, F., Sangiorgi, F., Schouten, S., 2020. Late Paleocene–early Eocene Arctic Ocean sea surface temperatures: reassessing biomarker paleothermometry at Lomonosov Ridge. Climate of the Past 16, 2381–2400.
Sridhar, P.N., Ali, M.M., Vethamony, P., Babu, M.T., Ramana, I.V., Jayakumar, S., 2008. Seasonal occurrence of unique sediment plume in the Bay of Bengal. Eos 89, 22. https://doi.org/10.1029/2008EO030002.
Tang, X., Naafs, B.D.A., Pancost, R.D., Liu, Z., Fan, T., Zheng, Y., 2021. Exploring the influences of temperature on "H-shaped" glycerol dialkyl glycerol tetraethers in a stratigraphic context: evidence from two peat cores across the late Quaternary. Frontiers in Earth Science 8, 1–7.
Tierney, J.E., Russell, J.M., 2009. Distributions of branched GDGTs in a tropical lake system: implications for lacustrine application of the MBT/CBT paleoproxy. Organic Geochemistry 40, 1032–1036.
Usman, M.O., Kirkels, F.M.S.A., Zwart, H.M., Basu, S., Ponton, C., Blattmann, T.M., Ploetze, M., Haghipour, N., McIntyre, C., Peterse, F., Lupker, M., Giosan, L., Eglinton, T.I., 2018. Reconciling drainage and receiving basin signatures of the Godavari River system. Biogeosciences 15, 3357–3375.
van der Voort, T.S., Hagedorn, F., McIntyre, C., Zell, C., Walthert, L., Schleppi, P., Feng, X., Eglinton, T.I., 2016. Variability in ^{14}C contents of soil organic matter at the plot and regional scale across climatic and geologic gradients. Biogeosciences 13, 3427–3439.
van Helmond, N.A.G.M., Quintana Krupinski, N.B., Lougheed, B.C., Obrochta, S.P., Andrén, T., Slomp, C.P., 2017. Seasonal hypoxia was a natural feature of the coastal zone in the Little Belt, Denmark, during the past 8 ka. Marine Geology 387, 45–57.
Vonk, J.E., van Dongen, B.E., Gustafsson, Ö., 2008. Lipid biomarker investigation of the origin and diagenetic state of sub-arctic terrestrial organic matter presently exported into the northern Bothnian Bay. Marine Chemistry 112, 1–10.
Weijers, J.W.H., Schouten, S., van den Donker, J.C., Hopmans, E.C., Sinninghe Damsté, J.S., 2007a. Environmental controls on bacterial tetraether membrane lipid distribution in soils. Geochimica et Cosmochimica Acta 71, 703–713.
Weijers, J.W.H., Schefuß, E., Schouten, S., Sinninghe Damsté, J.S., 2007b. Coupled thermal and hydrological evolution of tropical Africa over the last deglaciation. Science 315, 1701–1704.
Xie, S., Liu, X.-L., Schubotz, F., Wakeham, S.G., Hinrichs, K.-U., 2014. Distribution of glycerol ether lipids in the oxygen minimum zone of the Eastern Tropical North Pacific Ocean. Organic Geochemistry 71, 60–71.
Yu, M., Eglinton, T.I., Haghipour, N., Montluçon, D.B., Wacker, L., Wang, Z., Jin, G., Zhao, M., 2019. Molecular isotopic insights into hydrodynamic controls on fluvial suspended particulate organic matter transport. Geochimica et Cosmochimica Acta 262, 78–91.
Zell, C., Kim, J.-H., Abril, G., Sobrinho, R., Dorhout, D., Moreira-Turcq, P., Sinninghe Damsté, J., 2013a. Impact of seasonal hydrological variation on the distributions of tetraether lipids along the Amazon River in the central Amazon basin: implications for the MBT/CBT paleothermometer and the BIT index. Frontiers in Microbiology 4, 1–14.
Zell, C., Kim, J.-H., Moreira-Turcq, P., Abril, G., Hopmans, E.C., Bonnet, M.-P., Sobrinho, R.L., Damsté, J.S.S., 2013b. Disentangling the origins of branched tetraether lipids and crenarchaeol in the lower Amazon River: implications for GDGT-based proxies. Limnology and Oceanography 58, 343–353.